We are IntechOpen, the world's leading publisher of Open Access books
Built by scientists, for scientists

6,900
Open access books available

185,000
International authors and editors

200M
Downloads

154
Countries delivered to

Our authors are among the

TOP 1%
most cited scientists

12.2%
Contributors from top 500 universities

CLARIVATE ANALYTICS

BOOK CITATION INDEX

INDEXED

WEB OF SCIENCE™

Selection of our books indexed in the Book Citation Index
in Web of Science™ Core Collection (BKCI)

Interested in publishing with us?
Contact book.department@intechopen.com

Numbers displayed above are based on latest data collected.
For more information visit www.intechopen.com

The Thermo-mechanical Behavior in Automotive Brake and Clutch Systems

Abdullah M. Al-Shabibi
Sultan Qaboos University
Oman

1. Introduction

Automotive brakes and clutches involve bodies that are in contact and move relative to each other. Typically in the clutch, the contacting bodies take the shape of an axisymmetric disk. As similar as the contacting parts may be from system to system, their functions often vary. While they are used to decelerate or stop the motion of a rotating disk in the automotive brake, in the clutch system they are a mean of transmitting motion between two rotating parts. In the brake system the contact usually takes place between a rotating disk and a stationary friction pad. In the clutch system, however, the contacting disks are rotating at relative speeds and the contact results in a sliding motion over a short period of time till the two bodies are at the same speed. The length of the sliding motion depends on the amount of contact pressure applied, as well as the friction coefficient. The contact engagement in these systems takes place between the friction material of the friction disk and a steel surface.

The main problem associated with these types of systems is the variation of contact pressure distribution during engagement, which leads to areas of high-pressure concentration. As a result of sliding motion and friction, areas of high heat generation or hot spots may result which can in turn damage the contact surfaces. The damage can take different forms such as variation in the contacting disk thickness and surface cracks. The variation in disk thickness is expressed as disturbance to the applied load resulting in a low frequency vibration. Overheating of materials at the contact points, on the other hand, can lead to material degradation, which effectively reduces the lifetime of the effected system. Fig. 1 shows an example of hot spots patterns found in a clutch disk. The problem of hot spots has imposed design constraints to the brake and clutch systems in the past. Recently, it has become crucial to investigate the problem of hot spots promoted by the use of new materials and design improvements. The main objective of these investigations are to, if at all possible, completely eradicate the hot spots. This requires identification and examination of the parameters responsible for hot spots and simulation of the engagement process.

The sliding motion from the contact lasts for a short period of time that might not exceed half of a second, as is the case in the clutch system. Considering the short time of engagement the transient solution is indeed the key to understanding the process of hot spot formation. This will help to recognize how the problem fields, such as the temperature and the contact pressure evolve with time, in addition, to determine the possibility of material yielding through the computation of thermal stresses. Furthermore, design sensitivity analysis can be carried out with the availability of a transient solution.
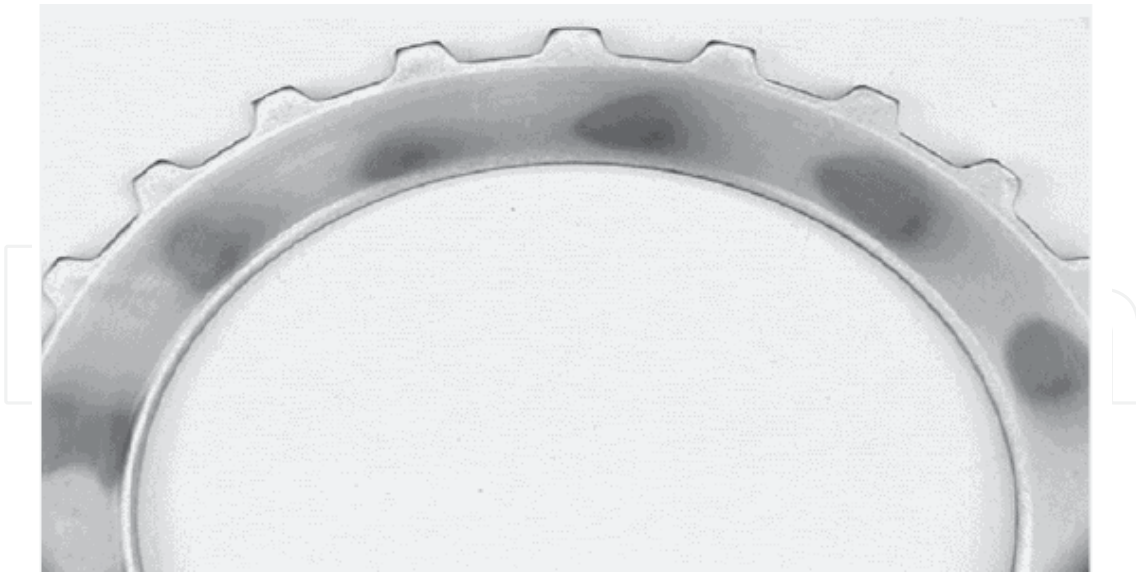
Fig. 1. Hot spot as it appears on a clutch desk.

1.1 Automotive brake and clutch system

There are two types of automotive clutch systems: wet and dry clutches. Dry clutch is typically used in a car with a manual transmission and its function is to connect the engine to the transmission. There are three main parts that make up the dry clutch: a flywheel, and clutch and pressure plates. The flywheel is connected to the engine whereas the clutch plate is connected to the transmission through a shaft. The flywheel and the clutch plate are engaged by pushing the pressure plate against the clutch disk, which in turn is pressed against the flywheel. This locks the engine to the transmission input's shaft, causing them to rotate at the same speed. The wet clutches, on the other hand, are used with the automatic transmission and they involve fluid flow across the contacting surfaces. They are used to engage different gears to the shaft transmitting the engine's rotation. The wet clutch consists of a pressure plate, pack of discs and an endplate. The disc pack is mounted between the pressure and end plates and consists of friction and steel disks. There are two types of friction disks that are commonly used in manufacturing the wet clutch system: single and double-sided friction disks. In the first, the friction material is applied to one side of a steel core, whereas, in the second, the friction material is layered on both sides of the steel core. For the case where double-sided friction disks are used, disc pack consists of alternating layers of friction and steel plates. Friction plates are splined on the inside, where they are locked to one of the gears. The steel plates, on the other hand, are splined on the outside, where they are locked to the clutch housing that transmits the engine's rotation. Grooves are also found on the surface of the friction disk that provides passages for the coolant fluids. The coolant fluid is used to cool down the contact interface, which also helps stabilizing the friction coefficient.

Similarly, there are two kinds of automotive brake systems that are commonly used in the automotive industry: disk and drum brakes. Most of the cars have disk brake on their front wheels and it composes of two friction pads, a steel disk mounted to the wheel hub and a caliper, which contains a piston. Disk brake operates through engaging the two pads in contact with the rotating steel disk. The steel disk contains a set of vanes that provide cooling to the brake system. The drum brake, on the other hand, consists of a steel drum,

hydraulic actuators and two brake shoes lined with a friction material. The hydraulic actuators are used to push the brake shoes against the brake drum.

1.2 Frictionally excited thermoelastic instability (TEI)

When two bodies are in contact and sliding relatively, frictional heat generation causes thermoelastic distortion that, in turn, modifies the initial contact pressure distribution. This feedback process is found to be unstable when the sliding speed exceeds a certain critical value. This phenomenon was first identified and explained by Barber (1967,1969) and was called "frictionally excited thermoelastic instability" or TEI. A microscopic disturbance in the contact pressure can grow resulting in areas of high-pressure concentrations and subsequently creating areas of high heat generations or 'hot spots'. Hot spots have been reported in a number of mechanical systems such as mechanical seals, aircraft brakes, railways and automotive clutch and brake systems. This phenomenon has been investigated both theoretically and experimentally over the last four decades. An overview of these investigations is presented in the following two sections to provide a better understanding of the TEI problem.

1.3 Field observations and experimental works

Parker and Marshall (1948) were the first to report evidence of TEI in railway brakes. Barber (1968,1969) carried a theoretical and experimental investigation and provided an explanation for the TEI phenomenon. He noted that a thermoelastic deformation causes a widely spread contacting asperities to concentrate at one or more discrete contact areas which are smaller than the nominal area. When the effect of thermoelastic distortion exceeds that of wear, the contact area changes can become unstable. Regions of high contact subsequently become regions of high heat flux that penetrate into sliding bodies causing thermal damages such as thermal cracks. Sehitoglu (1983) provided an explanation for the development of surface cracking, in which he noted that constraint on free thermal expansion of the hot spot by relatively cooler surrounding material is responsible for the formation of thermal fatigue cracks. Evidence of thermal cracks has been observed in railway brakes (Dow (1980), Fec and Sehitoglu (1985)), mechanical seals (Netzel (1980), Kennedy and Karpe (1982)) and automotive brakes (Anderson and Knapp (1989). High temperatures are another consequence of the high local heat flux, which also has been reported in the railway brake (Van Swaay (1969), Ho et al. (1974), Wentenkamp and Kipp (1976), Van Swaay (1979), Hewitt and Musial (1979)).

Investigations have been carried out to improve the performance of the brake system primarily through lowering the surface temperatures. Ho et al. (1974) conducted an investigation concerning aircraft brake in an attempt to develop improved brake materials. They suggested a criterion for determining the number and thickness of brake disks, where the thermal diffusivity and the length of the braking cycle play a very important role. Lower surface temperatures can be achieved by using materials of high specific heat and density, and by maximizing the contact area. Santini and Kinnedy (1975) monitored the surface temperature in an aircraft disk brake during a drag test, during which the sliding speed drops to zero from some initial value within a certain period of time. They noticed the development of non-uniform contact areas that are constantly shifting.

Evidences of thermoelastic instability were also observed in automotive brake and clutch systems over the past three decades. High local temperatures are found responsible for thermal cracking in automotive brakes (Anderson and Knapp (1989)), resulting in brake

fade (Lee and Barber (1993)). Furthermore, heat flux fluctuation can lead to thermoelastic distortion in the form surface waviness, which is expressed as disturbance to the applied load resulting in a low frequency or sometimes known as *brake judder* (Kreitlow et al. (1985), Thomas (1988)). Lee and Barber (1993) conducted an experimental investigation to better understand the TEI mechanism in the brake system and to validate the theoretical approximation as far as the onset of instability is concerned. They observed non-uniformities in the temperature, which is a clear evidence of thermoelastic instability in the brake system. They also reported changes in the form of the dominant perturbation as temperature is increased. Zagrodzki (1990, 1991) reported thermoelastic instability in a multi-disk clutch that resulted in permanent distortion such as coning. Lee and Dinwiddie (1998) investigated the effect of various contact conditions on the heating patterns and judder characteristics of a disk brake using infrared camera technology and vibration measurements. They showed that modified brake materials based on the theory of thermoelastic instability, in which the critical speed is increased to achieve a more stable brake system, can lead to a better judder performance. A similar investigation was also conducted by Edward Little *at al.* (1998), in which they demonstrated that increasing thermal disk thickness variation is accompanied by increasing brake torque variation. Yi at al. (2001) conducted a series of drag tests to investigate the phenomenon of TEI in an automotive disc brake. They used Fast Fourier Transform method to determine the exponential growth rate for various hot spot numbers and critical speed. Their results for critical speed and number of hot spots showed good agreement with the numerical prediction.

1.4 Theoretical investigations

The study of the thermoelastic process over the last four decades has followed mainly three branches; the study of stability analysis or critical speed, steady state solution and transient behavior.

Stability analysis

Stability analysis is mainly about the determination of the critical speed. Dow and Burton (1972) were the first in this field and they examined the stability of a sinusoidal perturbation that can grow exponentially in time for a semi-infinite plane sliding on a rigid surface. Their study reveals that the perturbation is unstable above a certain value of a sliding speed and this speed is different for different wave numbers. The critical speed for the system is then determined by the speed at which the first perturbation grows unstable.

Later, Burton *et al.* (1973) investigated the problem of two straight Blades contacting along a straight common interface which has been developed geometrically from a two cylindrical tubes pressed against each other by a uniform pressure. They found that for materials contacting their own kind, instability would be seen only at high values of friction coefficient. On the other hand, if one cylinder is changed to an insulator and one to a conductor, the disturbance will almost be stationary relative to the conductor and almost all of the heat will go into it. The stability in this case has a strong dependence on the sliding speed and the critical speed is low.

These findings, however, are not consistent with experimental observations in which evidence of instability was reported for contacting materials of similar properties. Berry (1984) has noted instabilities over a wide range of speeds and loads with various material combinations including cases of similar materials. Burton (1973) later offered an explanation

for this in which he explained that surface films such as natural oxidation products would act as thermal insulator. These thin films can change the stability behavior leading to instability. If the perturbation has a high velocity with respect to the body containing the film, the thermal penetration is small and the film properties may dominate the system.

Heckmann and Burton (1977) have also studied the effect of frictional shear traction on the stability boundary that has previously been neglected. They applied this study to the case where one body is considered a nonconductor and concluded that the introduction of shear has little effect on the predicted critical speed. Later, Lee and Barber (1993) studied the effect of shear traction when both materials are deformable and thermal conductors. They have shown that there is a significant change in the predicted critical speed when both materials have thermal properties of the same order of magnitude. Whereas stable behavior is predicted for two materials of similar thermal properties when shear effect is neglected, the presence of shear effect is shown to lead to bounded values of critical speed.

In studies so far, the model of two semi-infinite layers have been adopted where critical speed predicted by this model is more conservative when compared to that observed experimentally for automotive brake systems (Kreitlow et al. (1985), Anderson and Knapp (1989)). Lee and Barber (1993) extended Burton's model to include the dimension effect by studying the stability of a finite thickness layer that slides between two half-planes. This geometry is typical in the disk brake system where a finite thickness disk slides against two pads. They concluded that there is a preferred wavelength for instability whereas in two half planes model the critical speed decreases monotonically with wavelength. The threshold of instability is characterized by an antisymmetric perturbation leading to hot spots at alternating positions on the two sides of the disk. Their results of critical speed are of the order of those observed experimentally. Later, Lee (2000) developed a one sided heating model for automotive drum brakes and found the stability behavior of this model is similar to that of antisymmetric model of two sided heating with a higher critical speed. He also concluded that thermal expansion and friction coefficients are the most influential properties. Hartsock and Fash (2000) have also considered the effect of the friction pads' thickness on the stability behavior of the two-sided heating model. They incorporated the thickness of the pads by appropriately modifying their elastic modulus. They showed that the critical speed for thick friction pads is close to Lee's prediction but fell below it for thin pads.

Lee's model gives a better representation for the critical speed yet the computational complexity precludes extending it for a more realistic geometry. This complexity has been overcome by Du (1997) through the use of the finite element method to discretize the problem in space and formulate a discrete eigenvalue problem for the TEI. He examined his approach by solving a simple problem of half-plane sliding against rigid, non-conductive surface. Later Yi (2001) extended the finite element approach to solve the problem of two sliding bodies of a finite thickness including the three-dimensional disk problem.

Steady state problem

Stability analysis can determine the critical speed and shape of the unstable mode, however, it falls short to determine the amplitude of the contact pressure and the temperature field. Steady state solution, on the other hand, can show the value of the maximum thermal stresses and temperature encountered by the TEI system. This part of the TEI problem has been the focus of a number of studies in the past. Burton et al. (1973) has obtained the steady state solution for a conductive body sliding on a rigid nonconductive body. They assumed a

configuration of contacting spots separated by regions where the surfaces are parted and used power series to determine the contact pressure distribution for such a spot. They concluded that the distribution of pressure in the contact zone is approximately given by a parabolic relationship and the magnitude of the maximum pressure is dependent upon contact loading and the ratio of the operating velocity to the critical velocity. Burton and Nerliker (1975) obtained the solution for two conducting semi-infinite plates using the same technique of power series representation for the contact pressure in the contact region. They found two configurations that satisfy the boundary conditions, one of which is unstable. Latter Barber (1976) solved the problem of axisymmetric geometry using harmonic potential function and found that his solution is converging much faster than that of Burton using power series.

Transient problem

Although the steady state solution can predict the maximum pressure encountered by the TEI systems, typically, the engagement in the automotive brake and clutch systems take place over a very short period of time that is not enough for the system to reach the steady state. The best presentation is then acquired by solving for the transient behavior. The presence of the time variable in the governing equations makes it harder to obtain the transient solution, compared to the effort acquired by the other two solutions.

The transient solution has been the focus of some studies in the past. Barber (1980) presented a solution for the transient thermoelastic contact of a sphere sliding on a rigid non-conducting plane, subject to a Hertzian approximation to the contact pressure distribution. The aim of this study was to describe the transient process where an initially small pressure disturbance develops into a condition of patch like contact. They concluded if the ratio between the initial contact radius and the radius achieved in the steady state is large enough, the initial reduction in radius is linear with time depending only upon the initial contact radius and thermal diffusivity. Later, Barber et al. (1985) used the same model to evaluate the effect of design and operating conditions on the maximum temperature reached in brake and showed that in the case of uniform deceleration, the duration of the stop is significant. If the stop is sufficiently small for hot spots to develop, the temperature is high. High temperature is also reached if the stop is sufficiently fast because of the high rate of heat generation. There exists an optimum between theses two extremes.

Azarkhin and Barber (1985) presented a transient solution for an elastic conducting cylinder sliding against a rigid non conducting half plane. They used Green's function developed by Barber and Martin-Moran (1982), in which the solution of a thermoelastic contact problem can be expressed as a double integral of the surface heat input or temperature in time and space. Their method allowed them to follow the transient behavior of the system until it approaches the steady state for some values of the initial contact width. They also showed if the width of the initial contact is sufficiently large, bifurcation will occur and their method is not suited to pursue this phase of the process because of computational time and accuracy considerations. They have been able to overcome these difficulties by using a volume rather than the surface representation of the variables. Their solution has proven to be more accurate in comparison to that given by the Hertzian approximation and also enables them to follow the process through bifurcation.

The analytical solution of the transient thermoelastic contact problems such as those mentioned above are limited to a number of ideal problems which involve approximate geometry developed from a practical application. They also involve an extensive

computational time to reach convergence in the solution. Finite element method is an attractive alternative in which the domain of the problem is divided into sub-domains resulting in a system of linear first order differential equations. Theses equations are then solved utilizing time integration. A number of researchers have adopted this approach to study the transient thermoelastic contact problems, investigating the effect of different boundary condition configurations on the solution. Optimal design is also sought in those solutions in which geometrical dimensions and material properties played a very important role.

Kinnedy and Ling (1974) used finite element method to simulate the thermoelastic instabilities in the high-energy disk brakes. They investigated the effect of different material parameters on the temperature distribution in an attempt to determine the most important parameters for safe and reliable brake performance. Axisymmetric models were developed for a single-pad and annular disk brakes and the effect of wear was incorporated in theses models by proposing a criterion followed from experimental observations. They concluded that lower temperature in the disk brake assembly could be achieved by increasing the conductivity, the volume and the heat capacity of the heat sink component. Day (1984, 1988) presented a finite element analysis for drum brakes to investigate the role that interface pressure and thermal effects play in brake performance. They indicated the interdependence of interface pressure, temperature and wear over the friction material rubbing surface. Day and Tirovie (1991) has also described how the pressure at the friction interface of a drum and disc brake varies due geometry and deformation of the brake components, predicting interface pressure distribution and surface temperatures. Other finite element simulation involves investigating the transient thermoelastic behavior in composite brake disks (Sonn et al. 1995, 1996). Composite disks have demonstrated a lower temperature and pressure distribution along the friction surfaces.

Finite element analysis has also been used to investigate the transient process in the clutch system. Zagrodzki (1990, 1991) presented the axisymmetric solution of the transient problem for a multi-disk clutch, showing the effect of the TEI on the thermal stresses. He concluded that the thermomechanical phenomena occurring on any friction surface strongly effect the other friction surfaces and the Young's modulus of the friction material is very important. By reducing the modulus, the undesirable thermomechanical effects can be reduced.

1.5 Geometric modeling developments of TEI system

Because of the complexity of the TEI problem, early investigation of the TEI relied on an approximate two-dimensional model. Presuming an axisymmetric shape for the contacting bodies, Fourier series decomposition can be used along the circumferential direction. This allows the treatment of each Fourier mode separately and simplifies the mathematical formulations of the problem, providing no intermittent contact is experienced along the circumferential direction. Furthermore, plane strain or stress approximation can be adopted for the variation along the radial direction, where for small wave numbers plane strain is used and vice versa. The first two-dimensional model was used by Burton (1973) to study the stability of two sliding half-planes developed geometrically from a mechanical seal consisting of two cylindrical tubes. The same model has been used to predict the onset of instability for automotive brake system. Lee and Barber (1993) introduced a more representative two-dimensional model, in which they include finite thickness effect of the steel disk found in the disk brake system. Due to the geometric complexity involves in this class of problem, finite element approach is a more appropriate tool to treat a more realistic

geometry. Principally, finite element method can be used to model any TEI problem regardless of its geometric complexity.

The two-dimensional model has proven to be effective in determining the onset of instability in the brake system. Yi and Barber (1999) showed that except for a relatively small number of spots, the two- dimensional model give a very good prediction for the critical speed and the dominant wave length. The two-dimensional model, however, accounts only for instability along the sliding direction. Evidence of instability has also been observed across the sliding direction. Furthermore, the dominant thermal effect is found to be independent of the cirumferential direction in some cases, in which axisymmetric solution can be adopted. This model has been used to model the variation of the problem fields along the radial direction for the brake (Kennedy and Ling (1974) and clutch (Zagrodzki (1990, 1991)) problems. For a non-axisymmetric solutions a complete three-dimensional model is needed.

1.6 Finite element simulation of transient behavior

A clutch or a brake engagement can be simulated through a direct computer simulation. A schematic diagram representing the finite element simulation is shown in Fig. 2, which involves solving two coupled problems at the same time. This is achieved by constructing two different models, the first of which is used to solve the thermoelastic problem to yield displacement field and contact pressure distribution. The other model is used to solve the
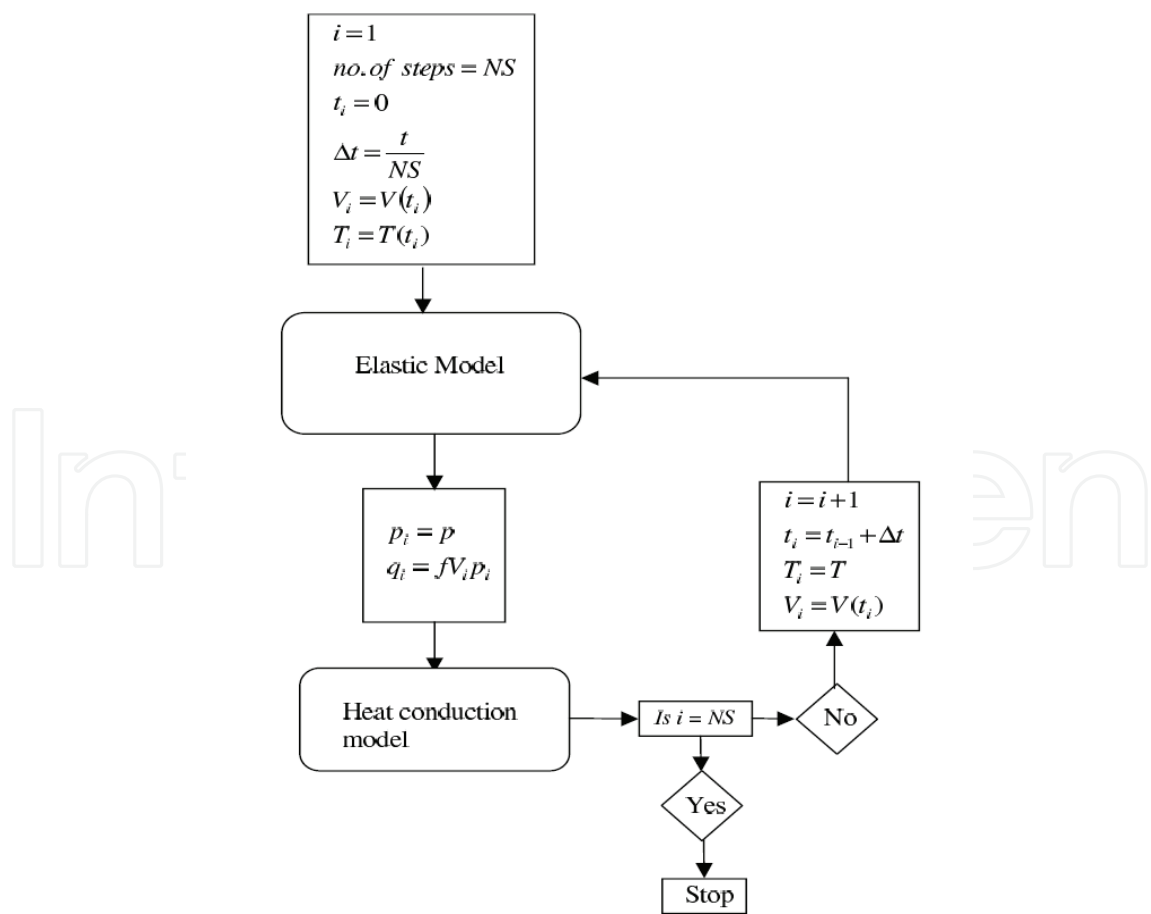

Fig. 2. Schematic diagram of FE simulation

transient heat conduction problem to account for the change in the temperature field during the simulated time step. The two models are coupled through the fact that the contact pressure from the first model is necessary in the second one to define the frictional heat flux. Moreover, the temperature field from the heat conduction model is needed for the computation of the contact pressure. This requires defining small time steps during which the contact pressures and sliding speed are assumed to remain constant. To acquire more accurate solutions, fine finite element mesh should be used which in turn requires the use of even smaller time steps to preserve numerical stability. This yields an extensive computational time, and although this is manageable for a two-dimensional problem it becomes extremely hard for a more realistic three-dimensional geometry.

2. Thermoelastic instability of half-plane sliding against rigid body

The aim of this section is to show how to analytically investigate the thermoelastic instability of sliding objects. A simple problem of a half-plane siding against a rigid body is considered. Burton's method of investigating TEI is to identify solutions of the perturbation problem of the exponential form

$$T(x,y,z,t) = e^{b_i t}\theta(x,y,z) , \tag{1}$$

where T is the temperature field in Cartesian coordinates x, y, z and t is time. Substitution of equation (1) into equations of heat conduction and thermoelasticity and the boundary conditions leads to an eigenvalue problem for the exponential growth rate b_i and the associated eigenfunction θ_i.

A general solution for the transient evolution of a perturbation at constant sliding speed can be written as an eigenfunction series

$$T(x,y,z,t) = \sum_{i=1}^{\infty} C_i e^{b_i t}\theta_i(x,y,z) , \tag{2}$$

where C_i is a set of arbitrary constants determined from the initial condition $T(x,y,z,0)$. It follows from equation (2) that if at least one eigenvalue is positive or complex with positive real part, the perturbation will grow without bounds and the system is unstable in the linear regime.

Fig. 3 shows the thermoelastic half plane $y > 0$ sliding against a rigid non-conducting body at speed V, which may be a function of time. The two bodies are infinite in extent in the x-direction and are pressed together by a uniform pressure p_0 applied at the extremities distant from the interface. Sliding friction occurs at the interface $y = 0$ with coefficient f, leading to the generation of frictional heat

$$q(x,t) = fVp(x,t) , \tag{3}$$

where $p(x,t)$ is the contact pressure. Since the lower body is non-conducting, all of this heat must flow into the thermoelastic half plane, resulting in the thermomechanically coupled boundary condition

$$q_y(x,0,t) = -K\frac{\partial T}{\partial y}(x,0,t) = fVp(x,t) , \tag{4}$$

where K is the thermal conductivity of the half plane.

This transient thermomechanical contact problem has a simple one-dimensional solution in which the contact pressure and the temperature field are independent of the x-coordinate. However, Burton *et al.* have shown that if the sliding speed is sufficiently high, this solution may be unstable, leading to the exponential growth of sinusoidal perturbations in temperature and pressure. For example, the contact pressure will then take the form

$$p(x,t) = p_0(t) + p_1 e^{bt} \cos(mx).$$ (5)

Eventually these perturbations will grow sufficiently large for separation to occur, after which the assumption of linearity will cease to apply
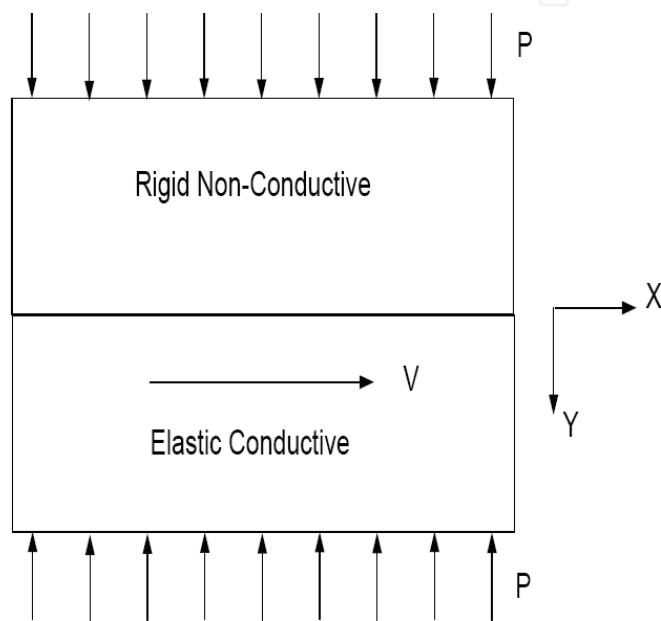
Fig. 3. Sliding contact of an elastic half-plane against a rigid plane surface

Solving for the exponential growth rate b proceeds in three steps. First, the transient heat equation (6) is solved for the temperature field that satisfies the thermal boundary conditions (4)

$$\frac{\partial^2 T}{\partial x^2} + \frac{\partial^2 T}{\partial y^2} = \frac{1}{k}\frac{\partial T}{\partial t},$$ (6)

where

$$k = \frac{K}{\rho c_p}$$

is the thermal diffusivity and K, ρ, C_p are the thermal conductivity, density, and specific heat respectively. The second step involves solving the thermoelastic problem for the displacement and stress components induced by the temperature field and satisfies the mechanical boundary conditions. Finally, the coupling term presented in the frictional heat flux is introduced to the two solutions.

Following Burton *et al.*, we consider cases in which the perturbation in the temperature field takes the sinusoidal form

$$T(x,y,t) = \theta(y)e^{bt}\cos(mx) .$$ (7)

Substitution in the transient heat conduction equation (6) yields the ordinary differential equation

$$\frac{d^2\theta}{dy^2} - \lambda^2\theta = 0$$ (8)

for $\theta(y)$, where

$$\lambda = \sqrt{m^2 + \frac{b}{k}}$$ (9)

Notice that λ is real for $b > -km^2$, which includes all cases of unstable perturbation ($b > 0$). Equation (8) has the two solutions $\theta = \exp(\pm\lambda y)$, but we restrict attention to the negative exponent, since the perturbed temperature field is assumed to decay as $y \to \infty$. We therefore obtain

$$T(x,y,t) = T_0 e^{-\lambda y + bt}\cos(mx),$$ (10)

where T_0 is an arbitrary constant.

The thermoelastic problem is solved for the displacements and stresses induced by the temperature field T as well as the mechanical boundary conditions. The particular solution corresponding to the temperature field is obtained by solving for the strain potential ψ through the following relation (Barber, 1993).

$$2\mu\underline{u} = \underline{\nabla}\psi$$ (11)

where

$$\nabla^2\psi = \frac{2\mu\alpha(1+\nu)}{1-\nu}T$$ (12)

and $\underline{u}$, μ, α, ν are the displacement vector, shear modulus, coefficient of thermal expansion and Poisson's ratio respectively. Substituting for T into the relations above, we obtain

$$\psi = \frac{2\mu\alpha(1+\nu)}{(1-\nu)(\lambda^2 - m^2)}T$$ (13)

The corresponding normal displacement and stress components are defined as followed

$$u_y = \frac{1}{2\mu}\frac{\partial\psi}{\partial y}$$ (14a)

$$\sigma_{yy} = -\frac{\partial^2\psi}{\partial x^2}$$ (14b)

$$\sigma_{xy} = -\frac{\partial^2 \psi}{\partial x \partial y} \tag{14c}$$

The particular solution presented above satisfies the field equation and it does not account for the mechanical boundary conditions of the problem where the stress components are required to decay to zeros away from the contact interface.

$$\sigma_{xx}, \ \sigma_{yy}, \ \sigma_{xy} \ \rightarrow \ 0 \quad as \quad y \rightarrow 0 \tag{15}$$

These boundary conditions are also found at interface or y = 0

$$u_y = 0 \tag{16a}$$

$$\sigma_{yy} = -p(x,t) \tag{16b}$$

$$\sigma_{xy} = 0 \tag{16c}$$

To satisfy the mechanical boundary conditions, the isothermal solutions A and D of Green and Zerna (1954) is superimposed to the particular solution. The corresponding normal displacement and stresses for the isothermal solutions are

$$u_y = \frac{1}{2\mu} \left\{ \frac{\partial \varphi}{\partial y} + y \frac{\partial \omega}{\partial y} - (3 - 4v)\omega \right\} \tag{17a}$$

$$\sigma_{yy} = -\frac{\partial^2 \varphi}{\partial x^2} + y \frac{\partial^2 \omega}{\partial y^2} - 2(1 - v)\frac{\partial \omega}{\partial y} \tag{17b}$$

$$\sigma_{xy} = -\frac{\partial^2 \varphi}{\partial x \partial y} + y \frac{\partial^2 \omega}{\partial x \partial y} - (1 - 2v)\frac{\partial \omega}{\partial x} \tag{17c}$$

where

$$\begin{aligned} \nabla^2 \varphi = 0 \\ \nabla^2 \omega = 0 \end{aligned} \tag{18}$$

φ and ω are chosen to satisfy the boundary conditions in (16)

$$\begin{aligned} \varphi = Ae^{-my} \cos mx \\ \omega = Be^{-my} \cos mx \end{aligned} \tag{19}$$

Substituting (13) into (14 a-c) and (19) into (17 a-c) and superimposing the two solutions yields,

$$u_y = \left\{ \frac{\alpha(1+v)\lambda}{(1-v)(\lambda^2 - m^2)} T_0 e^{-\lambda y + bt} \cos mx \right\} + \frac{1}{2\mu} mAe^{-my} \cos mx$$
$$+ \frac{1}{2\mu} \{my + (3 - 4v)\} mBe^{-my} \cos mx \tag{20a}$$

$$\sigma_{yy} = \frac{2\mu\alpha(1+\nu)m^2}{(1-\nu)(\lambda^2-m^2)} T_0 e^{-\alpha y + bt} \cos mx + m^2 A e^{-my} \cos mx \tag{20b}$$
$$+ \{my + 2(1-\nu)\} mB e^{-my} \cos mx$$

$$\sigma_{xy} = \frac{2\mu\alpha(1+\nu)m^2}{(1-\nu)(\lambda^2-m^2)} T_0 e^{-\alpha y + bt} \sin mx + m^2 A e^{-my} \sin mx \tag{20c}$$
$$+ \{my + (1-2\nu)\} mB e^{-my} \sin mx$$

The conditions (16a and 16c) are now used to define the constants A and B

$$A(t) = \frac{1}{m}\left\{ \frac{2\mu\alpha(1+\nu)T_0}{(1-\nu)(\lambda^2-m^2)} \left[2\nu(\lambda-m) + (m-2\lambda)\right] \right\} e^{bt} \tag{21a}$$
$$+ \frac{1}{m}\left\{ (1-2\nu)\frac{p_0}{m} \right\} e^{bt}$$

$$B(t) = \left\{ \frac{2\mu\alpha(1+\nu)T_0}{(1-\nu)(\lambda+m)} + \frac{p_0}{m} \right\} e^{bt} \tag{21b}$$

The condition (16b) is used to obtain the relationship between p_0 and T_0

$$p_0 = \frac{2\mu\alpha(1+\nu)m}{(\lambda+m)} T_0 \tag{21}$$

Finally, the coupling term of the frictional heat flux (4) is introduced which yielded the growth rate b as a function of the sliding speed V.

$$b(V) = k\left(\frac{mf\beta V}{K} - \frac{m^2}{2} - m\sqrt{\left(\frac{m}{2}\right)^2 + \frac{mf\beta V}{K}} \right) \tag{22}$$

where

$$\beta \equiv \frac{2\mu\alpha(1+\nu)}{1-\nu}$$

Fig. 4 shows the plot of the growth rate b as a function of the sliding speed V for two different wave numbers m. A critical speed exists for each wave number above which the sinusoidal perturbation will grow. Furthermore, different perturbation wave number holds different critical speed.

3. Finite element solution

In the previous section, the dominating eigenfunction has been identified. For a sliding speed above the critical value, the dominating eigenfunction is unstable and tends to
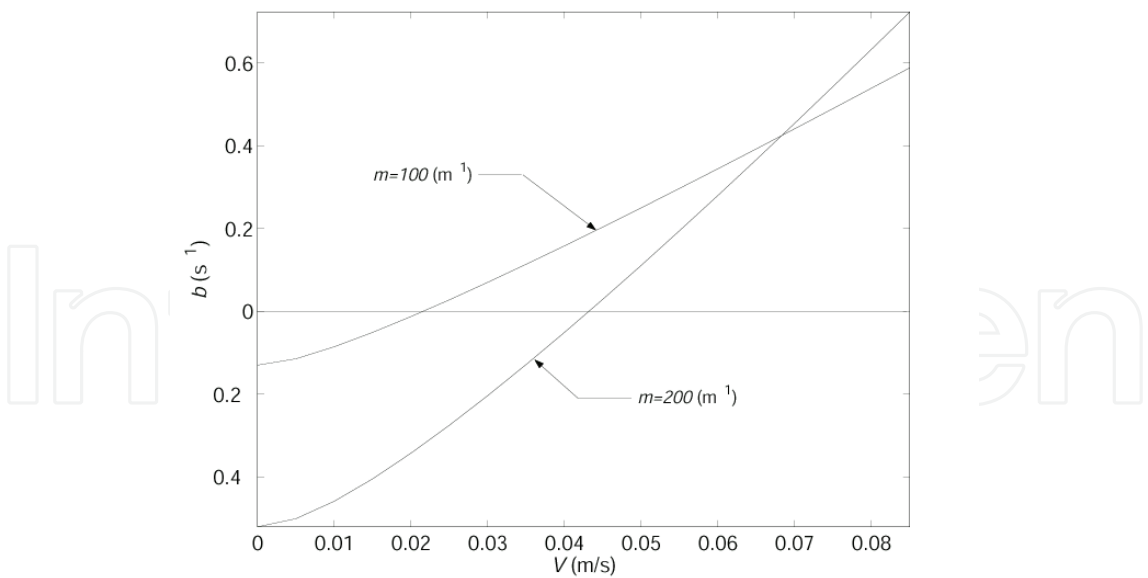
Fig. 4. The exponential growth rate b as a function of speed for two different wave numbers

dominate the solution. However, as the speed drops below the critical value, which is the case for a varying sliding speed, more eigenfunctions are needed in the expansion to maintain a reasonable amount of error in the solution. Obtaining the whole set of the eigenfunctions is a difficult task even for a simple geometry such as that considered in the previous section. This is mainly because of the coupling presented in the thermoelastic contact problem, which also involves solving two systems at the same time. Furthermore, treating a more realistic geometry add more complexity to the problem. Finite element method is a good alternative in which the problem is discretized in space. This will allow obtaining a set of eigenfunctions equivalent to the system's degrees of freedom. A more realistic geometry with practical material properties, similar to that found in the clutch problem can easily be incorporated in the finite element solution.

In this section, we should explore the method of governing a discrete eigenvalue problem considering a three dimensional model of two thermoelastic layers sliding relative to each other. This will involve solving for the exponential growth rate and the associated eigenfunction.

Fig. 5 shows two thermoelastic bodies Ω_1 and Ω_2 with surface boundaries Γ_1 and Γ_2, respectively, sliding at speed $V_1(t)$ and $V_2(t)$, which may be a function of time. The two bodies are infinite in extend in the x-direction and have a common contact interface $\Gamma_c = \Gamma_1 \bigcap \Gamma_2$ which is time independent.
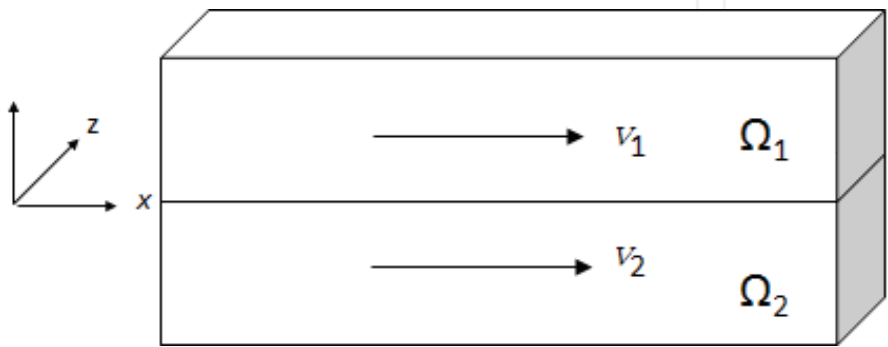

Fig. 5. Sliding contact of two elastic bodies.

Sliding friction occurs at the interface $y = 0$ with coefficient f, leading to the generation of frictional heat

$$q(x,z,t) = fVp(x,z,t),$$ (23)

where $p(x,z,t)$ is the contact pressure. The heat flow into the two bodies at the interface results in the thermomechanically boundary condition

$$q_y(x,0,z,t) = -\left(K^1 \frac{\partial T^1}{\partial y}(x,0,z,t) + K^2 \frac{\partial T^1}{\partial y}(x,0,z,t)\right) = fVp(x,z,t),$$ (24)

where K^1 and K^2 are thermal conductivity of Ω_1 and Ω_2 respectively. Furthermore, temperature continuity requires the temperature of the two bodies at the interface to be equal

$$T^1(x,0,t) = T^2(x,0,t).$$ (25)

Thermal insulation can be assumed for the surface boundary $\Gamma_1 \cup \Gamma_2 - \Gamma_c$

$$\frac{\partial T}{\partial n}(x,y,z,t) = 0, \quad (x,y,z \in \Gamma_1 \cup \Gamma_2 - \Gamma_c),$$ (26)

where n is the outward normal to the surface. This boundary condition is appropriate since $\Gamma_1 \cup \Gamma_2 - \Gamma_c$ are usually in contact with the atmospheric air and they hardly effect the transient solution.

Surface continuity requires the displacement field normal to the contact interface to be equal for the two bodies

$$u^1(x,0,t) = u^2(x,0,t).$$ (27)

3.1 Growth of a sinusoidal perturbation

Transient heat equation

Following Burton *et al.* (1973), we consider cases in which the perturbation in the temperature field takes the sinusoidal form and grows exponentially in time

$$T(x,y,z,t) = \Re\left\{\theta(y,z)e^{bt+jmx}\right\}.$$ (28)

This perturbation is then substituted in the transient heat conduction equation for body β ($\beta = 1, 2$) relative to frame of reference

$$\frac{\partial}{\partial x}\left(K^\beta \frac{\partial T^\beta}{\partial x}\right) + \frac{\partial}{\partial y}\left(K^\beta \frac{\partial T^\beta}{\partial y}\right) + \frac{\partial}{\partial z}\left(K^\beta \frac{\partial T^\beta}{\partial z}\right) = \rho^\beta c_p^\beta \left(\frac{\partial T^\beta}{\partial t} + V^\beta \frac{\partial T^\beta}{\partial x}\right),$$ (29)

to yield the ordinary differential equations

$$\frac{\partial}{\partial y}\left(K^\beta \frac{\partial \theta^\beta}{\partial y}\right) + \frac{\partial}{\partial z}\left(K^\beta \frac{\partial \theta^\beta}{\partial z}\right) - \left[K^\beta m^2 \theta^\beta + \rho^\beta c_p^\beta \left(jmV^\beta + b\right)\right]\theta^\beta = 0$$ (30)

for $\theta(y,z)$, where ρ^β and c_p^β are the density and specific heat of the material β. If the geometry is discretized by the finite element method, the instantaneous temperature field for each body can be characterized by a finite set of n^β nodal temperatures and it follows that there will be $n = n^1 + n^2$ terms in the eigenfunction series (2). To develop the eigenvalue problem, we first approximate the temperature function $\theta^\beta(y,z)$ of equation (28) in the form

$$\theta^\beta(y,z) = \sum_{i=1}^{n^\beta} N_i(y,z)\Theta_i^\beta , \qquad (31)$$

where Θ_i^β are nodal temperatures in body β and $N_i(y,z)$ are a set of n^β shape functions. Applying the weighted residual method to equation (30), we obtain the set of equations

$$\int_{\Omega^\beta} W_j\left(\frac{\partial}{\partial y}\left(K^\beta\frac{\partial\theta^\beta}{\partial y}\right) + \frac{\partial}{\partial z}\left(K^\beta\frac{\partial\theta^\beta}{\partial z}\right) - \left[K^\beta m^2\theta^\beta + \rho^\beta c_p^\beta\left(jmV^\beta + b\right)\right]\theta^\beta\right)d\Omega^\beta = 0 , \qquad (32)$$

where W_j is a set of linearly independent weighting functions. The second derivative in equation (32) is replaced with first derivative through integration by parts

$$-\int_{\Omega_\beta}\left(K_\beta\frac{\partial W_j}{\partial y}\frac{\partial\theta^\beta}{\partial y} + K_\beta\frac{\partial W_j}{\partial z}\frac{\partial\theta^\beta}{\partial z} - \left[K^\beta m^2\theta^\beta + \rho^\beta c_p^{\ \beta}\left(jmV^\beta + b\right)\right]W_j\theta^\beta\right)d\Omega_\beta$$

$$+\int_{\Omega_\beta}\left(K_\beta\frac{\partial}{\partial y}\left(W_j\frac{\partial\theta^\beta}{\partial y}\right) + K_\beta\frac{\partial}{\partial z}\left(W_j\frac{\partial\theta^\beta}{\partial z}\right)\right)d\Omega_\beta = 0 \qquad (33)$$

The second integral in (33) can then be replaced by a surface integral using Gauss' theorem to yield after considering the boundary condition (26)

$$-\int_{\Omega^\beta}\left(K^\beta\frac{\partial W_j}{\partial y}\frac{\partial\theta^\beta}{\partial y} + K^\beta\frac{\partial W_j}{\partial z}\frac{\partial\theta^\beta}{\partial z} - \left[K^\beta m^2 + \rho^\beta c_p^\beta\left(jmV^\beta + b\right)\right]W_j\theta^\beta\right)d\Omega^\beta$$

$$+\int_{\Gamma_c}\left(W_j q^\beta\right)d\Gamma_c \qquad (34)$$

where

$$q^\beta = -K^\beta\frac{\partial\theta^\beta(y,z)}{\partial n} , \quad \left(y,z \in \Gamma_c\right) \qquad (35)$$

Substituting (31) into (34) and using the same functions N_i as both shape and weighting functions, we obtain the matrix equation

$$\left(\mathbf{C}^\beta - m^2\mathbf{H}^\beta + jmV^\beta\mathbf{M}^\beta\right)\Theta^\beta + \mathbf{q}^\beta = b\mathbf{M}^\beta\Theta^\beta , \qquad (36)$$

where

$$C_{ji}^\beta = \int_{\Omega^\beta}\left(K^\beta\frac{\partial W_j}{\partial x}\frac{\partial W_i}{\partial x} + K^\beta\frac{\partial W_j}{\partial y}\frac{\partial W_i}{\partial y}\right)d\Omega^\beta ,$$

$$M_{ji}^\beta = \int\limits_{\Omega^\beta} \left(\rho^\beta c_p^\beta W_j W_i \right) d\Omega^\beta \,,$$

$$H_{ji}^\beta = \int\limits_{\Omega^\beta} \left(K^\beta W_j W_i \right) d\Omega^\beta \,,$$

and

$$q_j^\beta = \begin{cases} \int\limits_{\Gamma_c} \left(W_j q^\beta \right) d\Gamma_c, & j \in \Gamma_c \\ 0 & j \notin \Gamma_c \end{cases} \,,$$

Adding the matrix equations for the two bodies yields an assembled matrix equations for the whole system

$$\left(\mathbf{C} - m^2 \mathbf{H} + jm \mathbf{VM} \right) \mathbf{\Theta} + \mathbf{q} = b\mathbf{M\Theta} \,, \tag{37}$$

It might be more convenient to express (37) in the form

$$\left(\mathbf{C} - m^2 \mathbf{H} + jm \mathbf{VM} \right) \mathbf{\Theta} + \mathbf{Aq} = b\mathbf{M\Theta} \tag{38}$$

where

$$\mathbf{A} = \begin{bmatrix} \mathbf{I}_c \\ \mathbf{0} \end{bmatrix} \tag{39}$$

and $\mathbf{I_c}$ is the identity matrix of order $n_c \times n_c$ and n_c is the number of the contact nodes.

The thermoelastic problem

A second equation linking the contact pressure to the temperature distribution can be obtained from the finite element solution of the thermoelastic contact problem. We define a quasi-static displacement field in the form

$$u_x^\beta(x,y,z) = u^\beta(y,z)\sin(mx) \,, \tag{40a}$$

$$u_y^\beta(x,y,z) = v^\beta(y,z)\cos(mx) \,, \tag{40b}$$

$$u_z^\beta(x,y,z) = w^\beta(y,z)\cos(mx) \,. \tag{40c}$$

Time variable has been eliminated from the displacement field since the thermoelastic governing equations is time-independent. The displacement functions u, v and w are written in the discrete form

$$u^\beta(y,z) = \sum_{i=1}^{n^\beta} N_i(y,z) U_i^\beta \,, \tag{41a}$$

$$v^\beta(y,z) = \sum_{i=1}^{n^\beta} N_i(y,z)V_i^\beta \ , \tag{41b}$$

$$w^\beta(y,z) = \sum_{i=1}^{n^\beta} N_i(y,z)W_i^\beta \ , \tag{41c}$$

where U_i^β, V_i^β and W_i^β are the components of the nodal displacement vector $\mathbf{U}^\beta$. The potential energy for the body β can then be written

$$\Pi^\beta = \frac{1}{2}\int_{\Omega^\beta}\left(\boldsymbol{\varepsilon}^{\beta T}\boldsymbol{\sigma}^\beta - \boldsymbol{\varepsilon}_0^{\beta T}\boldsymbol{\sigma}^\beta\right)d\Omega^\beta - \int_{\Gamma_c} u_y{}^\beta p^\beta d\Gamma_c \tag{42}$$

where

$$\boldsymbol{\sigma} = \left\{\sigma_x, \sigma_y, \sigma_z, \tau_{xy}, \tau_{xz}, \tau_{yz}\right\} \ ,$$

$$\boldsymbol{\varepsilon} = \left\{\varepsilon_x, \varepsilon_y, \varepsilon_z, \gamma_{xy}, \gamma_{xz}, \gamma_{yz}\right\} \ ,$$

$$\boldsymbol{\varepsilon}_0 = \alpha T(x,y,z)\left\{1,1,1,0,0,0\right\} \ ,$$

are, respectively, the stress, strain and thermal strain vectors. The stress and strain are related by

$$\boldsymbol{\sigma}^\beta = \mathbf{D}^\beta\left(\boldsymbol{\varepsilon}^\beta - \boldsymbol{\varepsilon}_0^\beta\right) \tag{43}$$

Where

$$\mathbf{D} = \frac{E}{(1+v)(1-2v)}\begin{bmatrix} 1-v & v & v & 0 & 0 & 0 \\ v & 1-v & v & 0 & 0 & 0 \\ v & v & 1-v & 0 & 0 & 0 \\ 0 & 0 & 0 & (1-2v)/2 & 0 & 0 \\ 0 & 0 & 0 & 0 & (1-2v)/2 & 0 \\ 0 & 0 & 0 & 0 & 0 & (1-2v)/2 \end{bmatrix}.$$

Substituting (41a-c) into the strain-displacement relations, we obtain the discrete form of the strains as

$$\boldsymbol{\varepsilon}^\beta = \sum_{i=1}^{n}\mathbf{B}_i\mathbf{U}_i^\beta \ , \tag{44}$$

$$\boldsymbol{\varepsilon}_0^\beta = \sum_{i=1}^{n}N_i\Theta_i^\beta\left\{1,1,1,0,0,0\right\} \ , \tag{45}$$

where

$$\mathbf{B}_i = \begin{bmatrix} mN_i\cos(mx) & 0 & 0 \\ 0 & \dfrac{\partial N_i}{\partial y}\cos(mx) & 0 \\ 0 & 0 & \dfrac{\partial N_i}{\partial z}\cos(mx) \\ \dfrac{\partial N_i}{\partial y}\sin(mx) & -mN_i\sin(mx) & 0 \\ \dfrac{\partial N_i}{\partial z}\sin(mx) & 0 & -mN_i\sin(mx) \\ 0 & \dfrac{\partial N_i}{\partial z}\cos(mx) & \dfrac{\partial N_i}{\partial y}\cos(mx) \end{bmatrix}. \tag{46}$$

We then substitute (43-45) into (42) and perform the integrations. Minimizing the resulting expressions with respect to the nodal displacements U then yields the system of equations

$$\mathbf{K}^{\beta}\mathbf{U}^{\beta} = \mathbf{G}^{\beta}\mathbf{\Theta}^{\beta} + \mathbf{P}^{\beta}, \tag{47}$$

where

$$\mathbf{K}^{\beta} = \int_{\Omega^{\beta}} \tilde{\mathbf{B}}^{T}\mathbf{D}^{\beta}\tilde{\mathbf{B}}d\Omega^{\beta}; \quad \mathbf{G}^{\beta} = \int_{\Omega^{\beta}} \tilde{\mathbf{B}}^{T}\mathbf{D}\tilde{\mathbf{C}}d\Omega^{\beta}; \quad \mathbf{P}^{\beta} = \int_{\Gamma_c} \mathbf{N}pd\Gamma_c \tag{48}$$

and

$$\mathbf{B} = \begin{bmatrix} \tilde{B}_1 & \tilde{B}_2 & ... & \tilde{B}_{n^{\beta}} \end{bmatrix}; \quad \mathbf{C} = \begin{bmatrix} C_1 & C_2 & ... & C_n \end{bmatrix}; \quad \mathbf{N} = \begin{bmatrix} N_1 & N_2 & ... & N_{n^{\beta}} \end{bmatrix} \tag{49}$$

with

$$\tilde{\mathbf{B}}_i = \begin{bmatrix} mN_i & 0 & 0 \\ 0 & \dfrac{\partial N_i}{\partial y} & 0 \\ 0 & 0 & \dfrac{\partial N_i}{\partial z} \\ \dfrac{\partial N_i}{\partial y} & -mN_i & 0 \\ \dfrac{\partial N_i}{\partial z} & 0 & -mN_i \\ 0 & \dfrac{\partial N_i}{\partial z} & \dfrac{\partial N_i}{\partial y} \end{bmatrix}; \quad \tilde{C}_i = N_i \begin{Bmatrix} 1 \\ 1 \\ 1 \\ 0 \\ 0 \\ 0 \end{Bmatrix}. \tag{50}$$

Adding the matrix equations for the two bodies yield an assembled matrix equations for the whole system

$$\mathbf{KU} = \mathbf{G\Theta} + \mathbf{P}, \tag{51}$$

The unknown nodal displacements can be eliminated from the linear algebraic equations (51) to yield a system of equations for $\mathbf{P}_c$ in terms of $\tilde{\mathbf{\Theta}}$ which can be written in the symbolic form

$$\mathbf{P_c} = \mathbf{L\Theta} \tag{52}$$

The frictional heating relation $\mathbf{q_c} = fV\mathbf{p_c}$ and equations (38, 52) can then be used to eliminate $\mathbf{p_c}$, $\mathbf{q_c}$, leading to the generalized linear eigenvalue equation

$$\left(fV\mathbf{AL} - \mathbf{C} - m^2\mathbf{H} + jm\mathbf{VM} \right)\mathbf{\Theta} = b\mathbf{M\Theta} . \tag{53}$$

If the eigenvalues and eigenfunctions of this equation are denoted by b_k, $\hat{\Theta}_i^k$ respectively, a general solution for the evolution of the nodal temperatures $\Theta_i(t)$ at constant speed can be written as

$$\Theta_i(t) = \sum_{k=1}^{n} C_k \hat{\Theta}_i^k e^{b_k t} , \tag{54}$$

where the constants C_k are to be determined from the initial conditions.

4. Results for axisymmetric geometry

Critical speed corresponds to the sliding speed at which the exponential growth rate b is equal to zero. In the two-dimensional model of half plane sliding on a rigid surface, there exists one eigenmode that has the potential of becoming unstable beyond a certain value of the sliding speed. In the three-dimensional model of two axisymmetric disks, however, the growth rate is a complex number except for the axisymmetric or banding mode corresponding to $m = 0$.
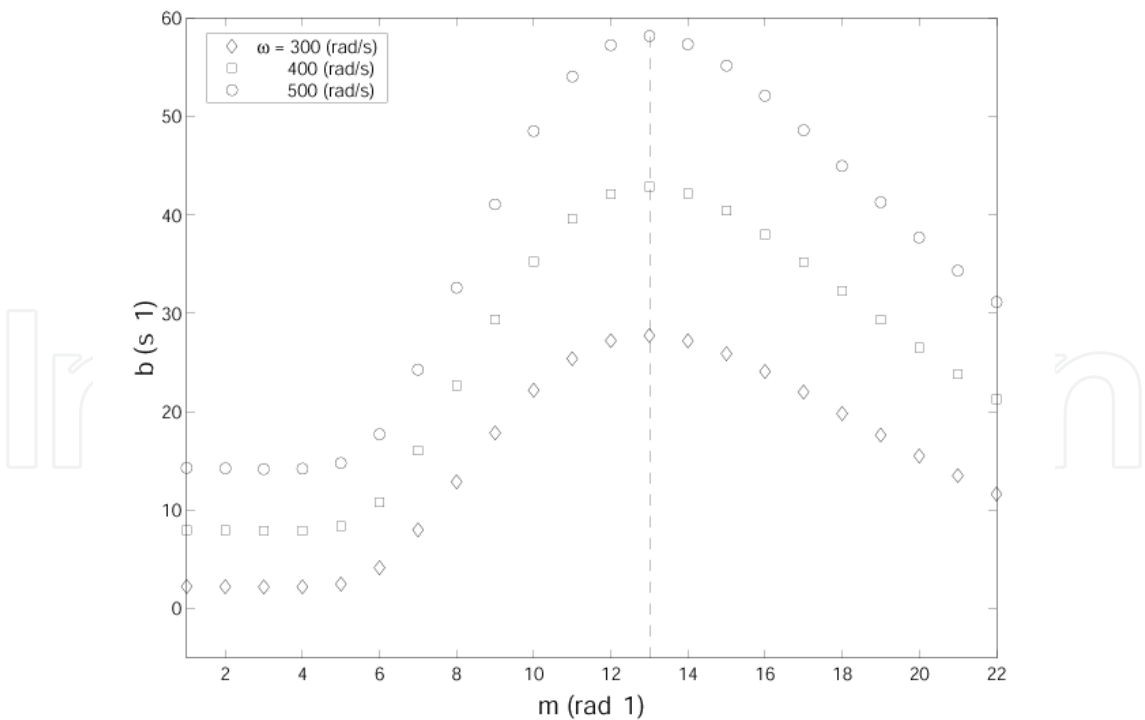

Fig. 6. Exponential growth rate of the dominating eigenmode as a function of wave number m for different operating speeds

Figure 6 shows the exponential growth rate of the dominating mode for each Fourier wave number and it can seen that, $m=13$ will grow faster than the other modes and it is therefore

anticipated the transient behavior of the system will be dominated by this Fourier mode. This especially true for the case where the sliding speed is constant. The stability of the system is determined by the wave number with the lowest critical speed. Unlike equation (22) where the critical speed increases monotonically with the wave number, there is a preferred wave number for the critical speed. Furthermore, there are more than one eigenmode that has the potential of becoming unstable depending on the value of the operating speed. The critical speed for each wave number m is determined by the speed at which the first eigenmode becomes unstable.

For each wave number m, there are n numbers of eigenmodes corresponding to the number of nodes used in the finite element model. Depending on the sliding speed, some of these eigenfunctions can be unstable. It is anticipated that the eigenfunction with the highest growth rate to dominate the transient process and the final solution is expected to take the shape of this eigenfunction. The dominating eigenmode for temperature in the contact surface is shown in Fig. 7 for m=13.
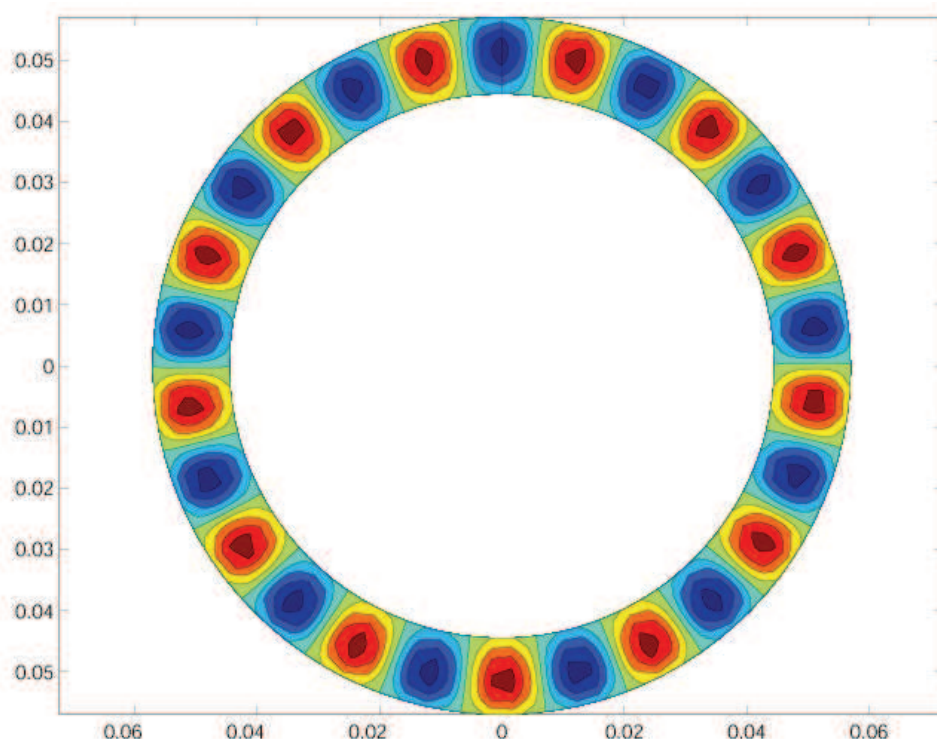

Fig. 7. Dominant eigenmode for the temperature in the contact surface for m = 13

5. Conclusion

This chapter shade some light on the thermomechanical behavior of automotive brake and clutch systems. The coupling between the thermoelastic problem and the thermal heat equation was found to result in the so called thermoelastic instability when the sliding speed is high enough. The first part of this chapter gave a historical literature review on the advancements that have been made in the area of thermoelastic instability. The research on this regard has mainly followed three streams, the stability analysis, the transient behavior and the steady state solution. Two approaches of investigating the thermelastic instability

have been presented, the analytical approach which is only possible for simplified geometries such as half-plane sliding against rigid body and the finite element approach which can accomedate a more complex geometries like those found in real brake and clutch systems.

6. References

Anderson, A.E. & Knapp, R.A. (1989), Hot spotting in automotive friction systems, Int. Conf. On wear of materials, Vol., 2, pp. 673-680

Azarkhin, A. & Barber, J.R. (1985), Transient thermoelastic contact problem of two sliding half-planes, Wear, Vol., 102, pp. 1-13

Barber, J.R. (1967), The influence of thermal expansion on the friction and wear process, Wear, Vol., 10, pp. 155-159

Barber, J.R. (1969), Thermoelastic instabilities in the sliding of conforming solids, Proc. Roy. Soc., Vol., A312, pp. 381-394

Barber, J.R. (1976), Some thermoelastic contact problems involving frictional heating, Q. J. Mech. Appl Math, Vol., 29, pp.1-13

Barber, J.R. (1980), The transient thermoelastic contact of a sphere sliding on aplane, Wear, Vol., 59, pp. 21-29

Barber, J.R. & Martin-Moran, C.J. (1982), Green's functions for transient thermoelastic contact problems for the half-plane, Wear, Vol., 79, pp. 11-19

Barber, J.R.; Beamond, T.W.; Waring, J.R. & Pritchard, C. (1985), Implications of thermoelastic instability for the design of brakes, J. Tribology, Vol., 107, pp. 206-210

Barber, J.R. (1992), Elasticity, Kluwer Academic Publisher

Berry, G.A. & Barber, J.R. (1984), The division of frictional heat – A guide to the nature of sliding contact, ASME J. Tribology, Vol., 106, pp. 405-415

Burton, R.A.; Nerlikar, V. & Kilaparti, S.R. (1973), Thermelastic instability in a seal-like configuration, Wear, Vol., 24, pp. 177-188

Burton, R.A. (1973), The role of insulating surface films in frictionally excited thermoelastic instabilities, Wear, Vol., 24, pp. 189-198

Burton, R.A.; Kilaparti, S.R. & Nerlikar, V. (1973), A limiting stationary configuration with partial contacting surfaces, Wear, Vol., 24, pp. 199-206

Carslaw, H.S. & Jaeger, J.C. (1959), Conduction of Heat in Solids, Oxford: Clarendon

Day, A.J.; Harding, P.R.J. & Newcomb, T.P. (1984), Combined thermal and mechanical analysis of drum brakes, Proc. Instn. Mech. Engrs., 198D(15), pp. 287-294

Day, A.J. (1988), An analysis of speed, temperature, and performance characteristics of automotive drum brakes, Trans. ASME, J. Tribology, Vol., 110, pp. 298-305

Day, A.J.; Tirovic, M. & Newcomb, T.P. (1991), Thermal effects and pressure distributions in brakes, Proc. Instn. Mech. Engrs, Vol., 205, pp. 199-205

Dow, T.A. & Burton, R.A. (1972), Thermoelastic instability of sliding contact in the absence of wear, Wear, Vol., 19, pp. 315-328

Dow, T.A. (1980), Thermoelastic effects in brakes, Wear, Vol., 59, pp. 213-221

Du, S.; Zagrodzki, P.; Barber, J.R. & Hulbert, G.M. (1997), Finite element analysis of frictionally-excited thermoelastic instability, J. Thermal stresses, Vol., 20, pp. 185-201

Fec, M.C. & Sehitoglu, H. (1985), Thermal-mechanical damage in railroad wheels due to hot spotting, Vol., 20, pp. 31-42

Green, A.E. & Zerna, W. (1954), Theoritical Elasticity, Clarendon Press, Oxford

Hartsock, D.L. & Fash, J.W. (2000), Effect of pad/caliper stiffness, pad thickness and pad length on thermoelastic instability in disk brakes, ASME J. Tribology

Heckmann, S.R. & Burton, R.A. (1977), Effects of shear and wear on instabilities caused by frictional heating in a seal-like configuration, ASLE Trans., Vol., 20, pp. 71-78

Hewitt, G.G. & Musial, C. (1979), The search for improved wheel materials, Inst. Mech. Eng., Int. Conf. on Railway Braking, York, p. 101

Ho, T.L.; Peterson, M.B. & Ling, F.F. (1974), Effect of frictional heating on braking materials, Wear, Vol. 26, pp. 73-91

Kennedy Jr., F.E. & Ling, F.F. (1974), A thermal, thermoelastic and wear simulation of a high energy sliding contact problem, J. Lub. Tech., Vol. 96, pp. 497-507

Kennedy Jr., F.E. & Karpe, S.A. (1982), Thermocracking of a mechanical face seal, Wear, Vol. 79, pp. 21-36

Kreitlow, W.; Schrodter, F. & Matthai, H. (1985), Vibration and hum of disc brakes under load, SAE 850079

Lee, Kwangjin & Barber, J.R. (1993), The effect of shear tractions on frictionally-excited Thermoelastic instability, Wear, Vol. 160, pp. 237-242

Lee, Kwangjin & Barber, J.R. (1993), Frictionally-excited Thermoelastic instability in automotive disk brakes, ASME Journal of Tribology, Vol. 115, pp. 607-614

Lee, Kwangjin & Dinwiddie, R.B. (1998), Conditions of frictional contact in disk brakes and their effects on brake judder, SAE 980598

Lee, K. (2000), Frictionally excited thermoelastic instability in automotive drum brakes, ASME J. Tribology, Vol. 122, 849-855

Netzel, J.P. (1980), Observations of thermoelastic instability in mechanical face seals, Wear, Vol. 59, pp. 135-148

Parker, R.C. & Marshall, P.R. (1984), The measurement of the temperature of sliding surfaces with particular reference to railway blocks, Proc. Inst. Mech. Eng., Vol. 158, pp. 209-229

Santini, J.J. & Kennedy, F.E. (1975), An experimental investigation of surface temperatures and wear in disk brakes, Lub. Eng., pp. 402-417

Sonn, H.W.; Kim, G.G.; Hong, C.S. & Yoon, B.I (1995), Transient thermoelastic analysis of composite brake disks, Journal of Reinforced Plastics and Composites, Vol. 14, pp. 1337-1361

Sonn, H.W.; Kim, G.C.; Hong, C.S. & Yoon, B.I. (1996), Axisymmetric analysis of transient thermoelastic behaviors in composite brake disks, Journal of Thermophysics and Heat Transfer, Vol. 10, pp. 69-75

Thoms, E. (1988), Disc brakes for heavy vehicles, Inst. Mech. Eng., Int. Conf. on Disc Brakes for Commercial Vehicles, C464/88, pp. 133-137

Van Swaay, J.L. (1979), Thermal damage to railway wheels, Inst. Mech. Eng., Int. Conf. on Railway Braking, York, p. 95

Wentenkamp, H.R. & Kipp, R.M. (1976), Hot spot heating by composite shoes, J. Eng. Ind., pp. 453-458

Yi, Y.; Barber, J.R. & Fash, J.W. (1999), Effect of geometry on thermoelastic instability in disk brakes and clutches, ASME J. Tribology, Vol. 121, pp. 661-666

Yi, Y.; Barber, J.R. & Zagrodzki, P. (2000), Eigenvalue solution of thermoelastic instability problems using Fourier reduction, Roy. Soc., Vol. A456, pp. 2799-2821

Zagrodzki, P. (1990), Analysis of thermomechanical phenomena in multidisc clutches and brakes, Wear, Vol. 140, pp. 291-308

Zagrodzki, P. (1991), Influence of design and material factors on thermal stresses in multiple disk wet clutches and brakes, SAE 911883
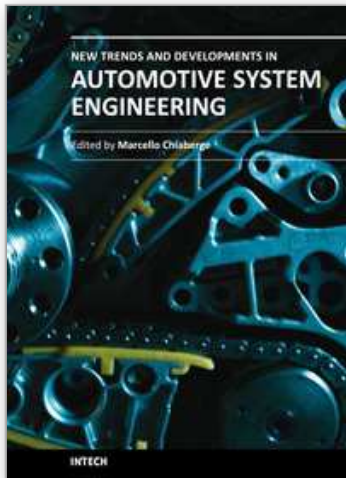
New Trends and Developments in Automotive System Engineering

Edited by Prof. Marcello Chiaberge

In the last few years the automobile design process is required to become more responsible and responsibly related to environmental needs. Basing the automotive design not only on the appearance, the visual appearance of the vehicle needs to be thought together and deeply integrated with the â€œpowerâ€ developed by the engine. The purpose of this book is to try to present the new technologies development scenario, and not to give any indication about the direction that should be given to the research in this complex and multi-disciplinary challenging field.

How to reference

In order to correctly reference this scholarly work, feel free to copy and paste the following:

Abdullah M. Al-Shabibi (2011). The Thermo-Mechanical Behavior in Automotive Brake and Clutch Systems, New Trends and Developments in Automotive System Engineering, Prof. Marcello Chiaberge (Ed.), ISBN: 978-953-307-517-4, InTech, Available from: http://www.intechopen.com/books/new-trends-and-developments-in-automotive-system-engineering/the-thermo-mechanical-behavior-in-automotive-brake-and-clutch-systems

INTECH
open science | open minds